Contribution from the Department of Chemistry,
Purdue University, West Lafayette, Indiana 47907

# Kinetics of Protonation of Palladium(II)–Tripeptide Complexes

JOHN C. COOPER, LOUIS F. WONG, and DALE W. MARGERUM*

*Received August 29, 1977*

Four sequential bond-dissociation steps occur when excess acid reacts with tripeptide ($L^-$) complexes of Pd(II). The dissociation starts at the carboxylate end with a fast reaction ($t_{1/2} < 10^{-3}$ s) and proceeds through intermediates where rapid protonation of the peptide oxygens occurs prior to Pd–N(peptide) bond cleavage. The limiting rate constants (25 °C, $\mu$ = 1 M) at high acid concentrations are 23.4 and 2.7 $s^{-1}$ for the stepwise dissociation of the two peptide nitrogens from palladium(II) triglycine. The fourth reaction, loss of the terminal amine coordination, is very slow. At lower acidities the second-order rate constant for $H^+$ attack on $Pd(H_{-2}GGG)^-$ with Pd–N(peptide) bond cleavage to give $Pd(H_{-1}GGG)$ is only one order of magnitude less than the corresponding reaction with $Ni(H_{-2}GGG)^-$. However, the equilibrium protonation constants are $10^{3.2}$ $M^{-1}$ for $[Pd(H_{-1}L)]/([Pd(H_{-2}L)^-][H^+])$ and $10^2$ $M^{-1}$ for $[PdL^+]/([Pd(H_{-1}L)][H^+])$, which are four and seven orders of magnitude smaller than the corresponding Ni(II) complexes, indicating the relatively high thermodynamic stability of Pd–N(peptide) bonding.

## Introduction

A number of divalent metal ions, including copper,[1,2] nickel,[2,3] and palladium[4,5] form N(peptide) bonds with deprotonation of the peptide group. Structure I shows a doubly

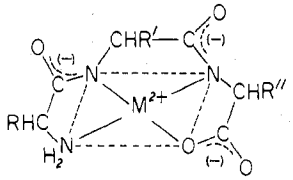

I

GGG, R = H; R′ = H; R″ = H
GGA, R = H; R′ = H; R″ = $CH_3$
GAG, R = H; R′ = $CH_3$; R″ = H
AGG, R = $CH_3$; R′ = H; R″ = H

deprotonated tripeptide complex.[6] We find that ionization of the peptide hydrogens occurs at pH 2–3 with palladium complexation, whereas the corresponding reactions with copper occur at pH 5–7 and with nickel at pH 7–9. In the present study the acid dissociation kinetics of palladium(II) triglycine, $Pd(H_{-2}GGG)^-$, are determined and compared with the reaction kinetics of $Cu^{II}$ and $Ni^{II}$ peptide complexes.[6-11] The $Pd^{II}$ reactions are much more sluggish than those of $Cu^{II}$ and do not undergo the changes in spin state (low spin to high spin) associated with the acid attack on $Ni(H_{-2}GGG)^-$. This permits a detailed examination of the $Pd(H_{-2}GGG)^-$ reaction path with acid, and four distinct steps are observed. Nevertheless, all steps except the last one are stopped-flow speed, indicative of hydrogen ion acceleration of the Pd–N(peptide) bond-dissociation rate.

A stopped-flow vidicon scanning spectrometer is used to help characterize the sequential reactions of the palladium(II)–triglycine complexes where the rate constants are separated by only about one order of magnitude. In addition, equilibrium circular dichroism–pH profiles of palladium(II) tripeptides, in which the chiral center is located in either the first, second, or third amino acid residue, are used to help assign the intermediate species observed in the acid dissociation reactions.

In previous studies of the protonation reactions of nickel(II)–peptide complexes a general mechanism was proposed to account for four different types of rate dependence which were observed.[11] This mechanism (eq 1 and 2) proposed the

$$MH_{-n}L + HX \underset{k_{-1}}{\overset{k_1}{\rightleftharpoons}} M(H_{-n}L)H + X \quad (1)$$

$$M(H_{-n}L)H \xrightarrow{k_2} M(H_{-n+1}L) \quad (2)$$

existence of appreciable concentrations of "outside protonated" species, $M(H_{-n}L)H$, where a proton adds without cleavage of the metal–N(peptide) bond. The behavior of the palladium(II) triglycine reactions supports this mechanism and gives additional evidence of outside protonated species. The most likely location of the proton in these species is that proposed in the structure of the protonated bis(glycylglycinato)cobaltate(III) complex,[12] in which the peptide oxygen is protonated. However, the kinetically reactive form may transfer the proton to the peptide nitrogen. One prediction of this general mechanism is that peptide complexes of the more sluggish metal ions would fail to show general acid catalysis and this is indeed the case for reactions of palladium(II) triglycine with various acids.

## Experimental Section

**Reagents.** Sodium tetrachloropalladate(II) was prepared from palladium(II) chloride and sodium chloride.[13] The resulting product was analyzed for palladium by adding excess sodium tetracyanonickelate(II) and titrating the free nickel with EDTA using murexide as an indicator[14] and for chloride potentiometrically with standard silver(I) solution. Anal. Calcd for $Na_2PdCl_4$: Pd, 36.2; Cl, 58.2. Found: Pd, 35.9; Cl, 57.7.

Triglycine (GGG), triglycinamide (GGGa), L-alanylglycylglycine (AGG), glycyl-L-alanylglycine (GAG), and glycylglycyl-L-alanine (GGA) were obtained as chromatographically pure compounds.

Palladium(II) tripeptide and triglycinamide solutions were freshly prepared for each set of experiments by the addition of solid sodium tetrachloropalladate(II) in a 1:1 mole ratio to a solution of the tripeptide or triglycinamide. Sodium hydroxide, $CO_2$ free, was added slowly to bring the solution to about pH 10 and then the solution was adjusted to the desired pH by the slow addition of dilute perchloric acid. Sodium perchlorate was used to maintain the ionic strength.

**Measurements.** Protonation–dissociation kinetics were measured spectrophotometrically at 25.0 ± 0.1 °C at several wavelengths, using a Durrum stopped-flow spectrophotometer with a 2.0-cm cell path. Kinetics data were obtained using an interfaced Hewlett-Packard 2115A computer.[15] All reactions in this study were run under pseudo-first-order conditions with excess acid or with buffered solutions. Equation 3 gives the rate expression for each of a series of sequential

$$\text{rate} = k_{obsd}[\text{Pd complex}] \quad (3)$$

reactions. Each rate constant is the average of at least three kinetic runs.

Hydrogen ion concentrations were determined from concentrations of standard acid solutions except those below $[H_3O^+]$ = 0.016 M where hydrogen ion concentrations were calculated from the pH measurements.

Circular dichroism (CD) measurements were made on a Cary Model 61 CD spectrophotometer at 25.0 ± 0.1 °C in a 1.00-cm cell. Results are reported as $\Delta\epsilon = \epsilon_L - \epsilon_R$ (based on $[Pd(II)]_{total}$) or ellipticity ($\theta$). The CD measurements to determine protonation constants for

0020-1669/78/1317-0261$01.00/0 

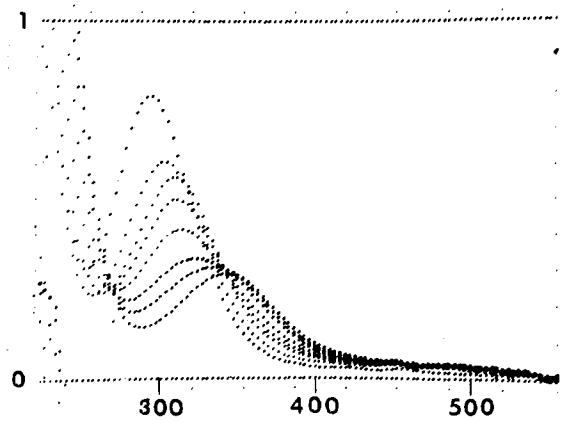


**Figure 1.** Spectral data from the vidicon stopped-flow system for the reaction of $Pd(H_{-2}GGG)^-$ with acid. Absorbance vs. wavelength reading from top to bottom at 300 nm for $Pd(H_{-2}GGG)^-$ and the species produced after 10, 100, 250, 500, 1000, 1500, and 5000 ms.

the palladium(II) tripeptides were made after equilibrating the solution for 5 days or more.

Resolution of sequential rate constants in the protonation kinetics studies was achieved by two different methods: (1) use of a nonlinear regression program NONLINR[16] for analysis of data spanning the time range of two sequential reactions observed at a wavelength of 300 nm, and (2) use of rapid-scan spectra to locate suitable isosbestics for following one reaction at a time.

The rapid vidicon-scanning spectrophotometer and data acquisition system used in this study are described elsewhere.[17,18]

## Results and Discussion

When solutions of $Pd(H_{-2}GGG)^-$ are mixed with acid there is an initial absorbance change (first reaction) which is complete within the stopped-flow dead time (5 ms). This is followed by three sequential first-order reactions (eq 4). The

$$Pd(H_{-2}GGG)^- \xrightarrow[\text{rapid}]{k_1} X \xrightarrow{k_2(\text{obsd})} Y \xrightarrow{k_3(\text{obsd})} Z \xrightarrow{k_4(\text{obsd})} H_2GGG^+ + Pd^{II} \quad (4)$$

second and third reactions overlap to some degree but each can be resolved into first-order rate constants which increase with the hydrogen ion concentration and reach limiting values at about 0.2 M $[H^+]$. At this acidity the half-lives are 30 ms for X and 270 ms for Y. The fourth observed reaction is very slow compared to the others and species Z has a half-life of several hours. The reactions are independent of $Cl^-$ except for the fourth reaction which becomes faster if excess chloride ion is added.

Rapid scan spectra (Figure 1) taken with the vidicon stopped-flow unit permitted wavelengths to be located so that the second reaction (corresponding to $k_2$) could be studied at an isosbestic point for the Y and Z species and the third reaction (corresponding to $k_3$) could be studied at an isosbestic point for X and Y. After locating the isosbestic points the reactions were run on the Durrum stopped flow at the appropriate wavelengths to give more precise rate constants.

The first three reactions of palladium(II) triglycine with acid were not affected by chloride ion. This was tested by removing $Cl^-$ by precipitation with stoichiometric amounts of $AgClO_4$ as well as by the addition of larger amounts of chloride ion. Thus, the magnitude of the rapid absorbance change and the values of $k_2$(obsd) and of $k_3$(obsd) were independent of chloride ion concentration. However, the fourth reaction was dependent on chloride ion and independent of hydrogen ion concentration. The $k_4$(obsd) value for $Pd(AGG)H^{2+}$ in 1 M $H^+$ and $2.4 \times 10^{-3}$ M $Cl^-$ was $7.7 \times 10^{-6}$ $s^{-1}$ and this rate constant became much larger in 0.025 M $Cl^-$. High $Cl^-$ concentrations caused the reactions to be much faster even at lower acidity and the $k_4$(obsd) value for $Pd(GGG)H^{2+}$ in 0.1 M $H^+$ and 0.4 M $Cl^-$ was $6.68 \times 10^{-3}$ $s^{-1}$. Similar rate behavior was observed using CD spectrophotometry to follow the slowest reaction of the palladium(II)–L-alanylglycylglycine complex with acid. All the CD signal was lost in this reaction and it is concluded that the fourth reaction involves the addition of $Cl^-$ and the loss of the amino-terminus-bound tripeptide.

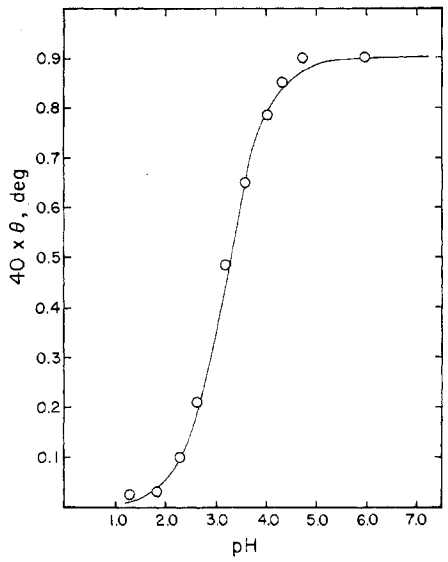


**Figure 2.** The pH dependence of the CD signal for the Pd–GGA complex at 338 nm: $6.0 \times 10^{-4}$ M $[PdGGA]_{total}$, $2.4 \times 10^{-3}$ M $[Cl^-]$, $\mu$ 1.0 M ($NaClO_4$). The solid line is calculated using log $K_H = 3.2$ for the formation of $Pd(H_{-1}GGA)$ from $Pd(H_{-2}GGA)^-$.

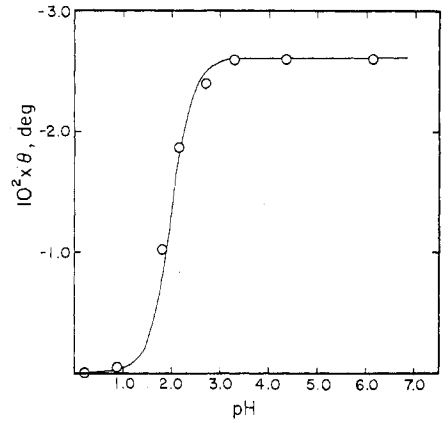


**Figure 3.** CD–pH profile for the Pd–GAG complex at 358 nm (isosbestic point for the first protonation): $6.0 \times 10^{-4}$ M $[PdGAG]_{total}$, $2.4 \times 10^{-3}$ M $[Cl^-]$, $\mu$ 1.0 M ($NaClO_4$). The solid line is calculated for the simultaneous addition of two protons to $Pd(H_{-1}GAG)$ using log $\beta_2 = 4.0$ where $\beta_2 = [Pd(GAG)H^{2+}]/([Pd(H_{-1}GAG)][H^+]^2)$.

**CD Studies to Identify the Reaction Sequence.** Equilibrium mixtures of palladium(II) tripeptides with variable $HClO_4$ concentrations at 1.0 M ionic strength ($NaClO_4$) in the presence of $2.4 \times 10^{-3}$ M $Cl^-$ were studied by the circular dichroism of the metal d → d transitions. The tripeptides contained two glycyl residues and one L-alanyl (chiral) residue which was located in either the first position (AGG), the second position (GAG), or the third position (GGA). The circular dichroic activity in the metal complex arises from the association of the chiral peptide residue with the metal center. The CD signal for the peptide itself appears at much lower wavelength than that of the metal complex. The variation of the CD signal with pH is shown for the Pd(II) complexes of GGA, GAG, and AGG in Figures 2, 3, and 4 for selected wavelengths.

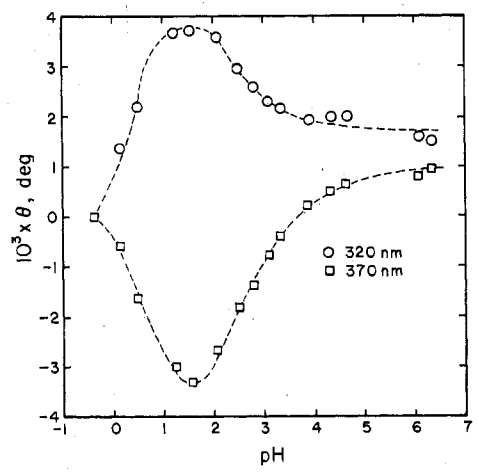


**Figure 4.** CD–pH profile for the Pd–AGG complex at 320 nm (○) and 370 nm (□): $6.0 \times 10^{-4}$ M $[PdGGA]_{total}$, $2.4 \times 10^{-3}$ M $[Cl^-]$, variable $\mu$ (1–3 M $NaClO_4$–$HClO_4$).

**Pd(II)–GGA.** The CD–pH profile corresponds to the addition of a single hydrogen ion to the complex causing a complete loss of the CD signal. The resolved value for log $K_H$ = 3.2 (obtained from plots of $\theta$ vs. $\Delta\theta/[H^+]$) is used to calculate the curve in Figure 2. The protonation constant of the carboxylate group of uncomplexed triglycine (to give $H_2GGG^+$) is $10^{3.2}$; however, in the complex, protonation of the carboxylate end must compete with Pd(II) chelation, so that a log $K_H$ value much lower than 3.2 would be expected if only the carboxylate group is protonated. Furthermore, if the proton adds to the carboxylate group there should not be a complete loss of the CD signal because the optically active group would still be near to the chromophoric center. Therefore, we conclude that the proton adds to a peptide nitrogen to give $Pd(H_{-1}GGA)$ as given in structure II where

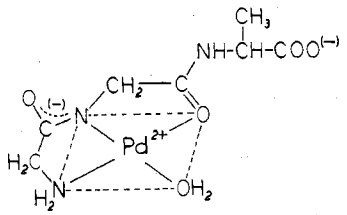

II

the last peptide oxygen is coordinated to the palladium. An additional proton would be expected to add to the carboxylate group in structure II but its log $K$ value must be less than 2.2 in order to give the observed fit in Figure 2. The lowering of the carboxylate log $K_H$ value would be due to the proximity of the Pd(II) center. We propose that the coordination in structure II corresponds to that in species Y in eq 4. Additional protons can be added to the complex below pH 2 without being observed in the CD measurements because the CD signal is already lost for GGA.

**Pd(II)–GAG.** Figure 3, the CD–pH profile for palladium(II) glycyl-L-alanylglycine at 358 nm (where there is a CD isosbestic point for the first protonation), gives an inflection at pH 2. However, the best fit of the CD–pH curve is for the addition of two protons simultaneously and the curve in Figure 3 is calculated for $\beta_2 = [Pd(GAG)H^{2+}]/([Pd(H_{-1}GAG)]\cdot[H^+]^2) = 1 \times 10^4$ $M^{-2}$. Once the second peptide nitrogen is protonated the carboxylate group also adds a proton as it is now well removed from the Pd(II) and hence becomes a more basic site. We propose that $Pd(GAG)H^{2+}$ corresponds to structure III. The chiral center is removed from the vicinity of Pd(II) and the CD signal due to the metal d–d transition

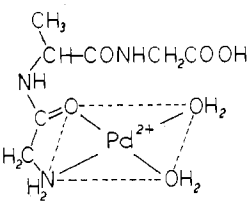

III

is completely lost. Structure III corresponds to species Z in eq 4. In order to observe the simultaneous addition of two protons the carboxylate group is not protonated until the second peptide nitrogen adds a proton to give $Pd(GAG)^+$ and hence the latter log $K_H$ value is 2 or less.

Observation of the CD spectra at other wavelengths (e.g., 342 nm) where there is no isosbestic for the first protonation (pH 3.2) shows evidence of the CD changes which can be attributed to protonation and reorganization of the coordination of groups distant from the chiral center (changes from structure I to structure II). Thus, the CD spectrum of Pd(II) GAG is sensitive to all changes of coordination with pH which affect the absorption spectrum up to and including the coordination adjacent to the chiral center. However, as soon as the coordinated groups adjacent to the chiral center are removed from the metal, the CD signal drops to zero.

**Pd(II)–AGG.** Figure 4 gives the CD–pH profile for palladium(II) L-alanylglycylglycine at CD maxima 320 and 370 nm. The magnitude of the CD signal observed for the Pd(II) AGG complex is approximately 10% of that observed for either the Pd(II)–GAG or Pd(II)–GGA complexes. The behavior of both CD–pH plots (λ 320 and 370 nm) can be interpreted using the data from the Pd(II) GGA and Pd(II) GAG cases.

The protonation of the first peptide group corresponding to the log $K_H$ found with Pd(II) GGA is reflected in the CD–pH plot at 370 nm which shows large changes around pH 3.2. At both 320 and 370 nm, additional changes below pH 2.5 are observed. However, this protonation equilibrium is masked by the final ligand dissociation equilibrium, resulting in apparent maxima or minima in CD intensity in the region of pH 1.5. This low-pH portion of the CD–pH plot at either wavelength represents the protonation and removal of the alanylpeptide segment from the metal center. This apparent log $K_H$ value, in accord with the inflection point of either curve at low pH, is about 0.4. The equilibrium represented by this value (eq 5) involves the protonation of the amine terminal

$$K_4 = \frac{[Pd(II)][H_2AGG^+]}{[Pd(AGG)H^{2+}][H^+]} \qquad (5)$$

after its dissociation from the Pd(II) center. This dissociation is required because there is a complete loss of CD signal. The products of this protonation and peptide dissociation at very low pH correspond to the products of the final step in eq 4. Hence, this $K_H$ value corresponds to $K_4/[Pd(II)]$ so that $K_4 \simeq 10^3$ at a chloride ion concentration of $2.4 \times 10^{-3}$ M. Again we can see that when a peptide group containing the chiral group is coordinated, protonation and rearrangements of distant groups can have an effect on the CD signal.

Circular dichroism spectroscopy was useful in correlating the stable protonated species found in equilibrium situations with those proposed as intermediates in the palladium(II) triglycine kinetics.

**Initial Absorbance Change with the $Pd(H_{-2}GGG)^-$ and $H^+$ Reaction.** There are significant differences between the absorbance of the $Pd(H_{-2}GGG)^-$ solution at pH 6 and the initial absorbances after mixing with acid ($\Delta A_0$ at 276 nm in Table I). This very rapid absorbance decrease corresponds to the first step in eq 4 and also is observed to a lesser degree at pH 3, where the subsequent $k_2$ (obsd) rate constant is

**Table I.** Protonation Reactions of Palladium(II) Triglycine[d]

| $[H^+]$, M | $\Delta A_0$[a] | $k_2$(obsd),[b] $s^{-1}$ | $k_3$(obsd),[c] $s^{-1}$ |
|---|---|---|---|
| 0.010 | 0.160 ± 0.002 | 14.6 ± 0.6 | 1.10 ± 0.02 |
| 0.015 | 0.158 ± 0.001 | 16.9 ± 0.7 | 1.28 ± 0.01 |
| 0.025 | 0.161 ± 0.001 | 18.9 ± 0.2 | 1.56 ± 0.01 |
| 0.050 | 0.165 ± 0.001 | 20.4 ± 0.2 | 1.95 ± 0.01 |
| 0.10 | 0.168 ± 0.001 | 22.5 ± 0.5 | 2.33 ± 0.01 |
| 0.20 | 0.170 ± 0.001 | 23.2 ± 0.5 | 2.56 ± 0.02 |
| 0.25 | 0.171 ± 0.001 | 22.3 ± 0.2 | 2.58 ± 0.01 |
| 0.30 | 0.172 ± 0.001 | 22.7 ± 0.9 | 2.60 ± 0.01 |
| 0.40 | 0.172 ± 0.002 | 23.5 ± 1.0 | 2.58 ± 0.04 |
| 0.50 | 0.173 ± 0.001 | 23.4 ± 0.4 | 2.52 ± 0.01 |

[a] Immediate absorbance decrease at 276 nm upon mixing with $HClO_4$. The $\Delta A_0$ value is the calculated $A_{initial}$ for $Pd(H_{-2}GGG)^-$ less the observed absorbances extrapolated to the time of mixing. [b] Actual $A_0 = 0.401$, λ 276 nm. [c] Actual $A_0 = 0.468$, λ 327 nm. [d] $\mu = 1.0$ M ($NaClO_4$), 25.0 °C, $[Pd(H_{-2}GGG)^-] = 5.0 \times 10^{-4}$ M. Observed rate constants are averaged from three or more runs. Error limits shown are standard deviations for replicate runs.

**Table II.** Protonation Reactions of the Palladium(II) Complex of Triglycinamide[c]

| Initial pH of Pd solution | Added $[H^+]$ | $\Delta A_0$[a] | $k_2'$(obsd),[b] $s^{-1}$ | $k_3'$(obsd),[b] $s^{-1}$ |
|---|---|---|---|---|
| 6.5 | 0.025 | 0.045 ± 0.005 | 42.3 ± 1.6 | 1.99 ± 0.02 |
| 6.5 | 0.0375 | 0.055 ± 0.004 | 47.2 ± 1.2 | 2.33 ± 0.02 |
| 6.5 | 0.050 | 0.058 ± 0.005 | 52.6 ± 1.4 | 2.44 ± 0.02 |
| 8.6 | 0.025 | 0.478 ± 0.003 | | |
| 8.6 | 0.0375 | 0.472 ± 0.005 | | |
| 8.6 | 0.050 | 0.479 ± 0.006 | | |

[a] $\Delta A_0$ is the theoretical initial absorbance minus extrapolated $A_0$ from absorbance vs. time data. [b] Resolved by a nonlinear regression procedure. [c] $\mu = 0.1$ M ($NaClO_4$), $t = 25.0$ °C, $[Pd(H_{-2}GGGa)]_{total} = 5.8 \times 10^{-4}$ M, $[H^+] = 0.025$–0.05 M ($HClO_4$). λ 282 nm. Observed rate constants are averages of three or more runs.

relatively small. There are several possible protonation sites which could accept a proton very rapidly. Outside protonation of the metal-peptide is one possibility and the leveling off of the values of $k_2$(obsd) at high acidity shown in Figure 4 tends to support this in accord with the mechanism in eq 1 and 2 observed for the reactions of $Ni(H_{-3}GGGG)^{2-}$ and $Ni(H_{-3}GGGamide)^-$. However, the carboxylate group also could be protonated and released from its coordination to $Pd^{II}$. We suggest that both processes occur with the formation of a hydrogen bonded outside protonation species as is postulated for $Ni(H_{-3}GGGG)^{2-}$.

In order to help resolve the source of the absorbance jump on mixing $Pd(H_{-2}GGG)^-$ with acid, the protonation reactions of the palladium(II) triglycinamide complex were studied. The $Pd(H_{-2}GGGa)$ complex loses a proton from the amide group to form $Pd(H_{-3}GGGa)^-$ with a $pK_a$ of 8.4.[19] There is a large spectral difference between $Pd(H_{-3}GGGa)^-$ and $Pd(H_{-2}GGGa)$. The $\Delta A_0$ values of $Pd(H_{-3}GGGa)$ at 282 nm upon mixing excess acid with solutions initially at pH 6.5 compared to mixing excess acid with solutions initially at pH 8.6 are given in Table II. There is very little absorbance change in the first instance and a large, very rapid absorbance change for solutions initially at pH 8.6. Clearly the initial absorbance change is due to cleavage of the terminal amide bonding to Pd(II) and not just to outside protonation of peptide oxygens. Since initial mixing of $Pd(H_{-2}G_3)^-$ with acid is accompanied by a similar absorbance jump we conclude Pd(II)–carboxylate bond breaking occurs. The smaller absorbance change ($\Delta A_0$) observed for the triglycine vs. triglycinamide case is because the triglycine reaction was followed at an isosbestic point away from the peak maximum whereas the triglycinamide reactions are followed at the peak maximum

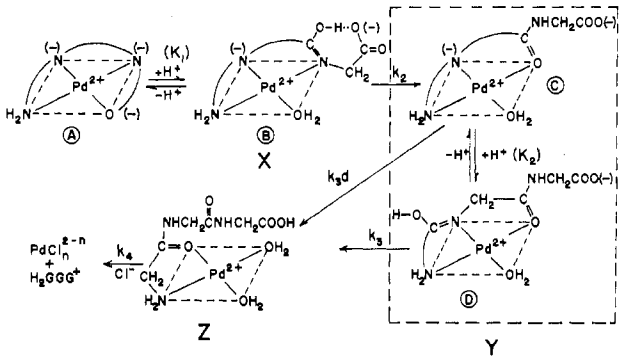


**Figure 5.** Proposed reaction mechanism for the acid decomposition of the Pd–GGG complex, where all the species shown can be present in appreciable concentrations.

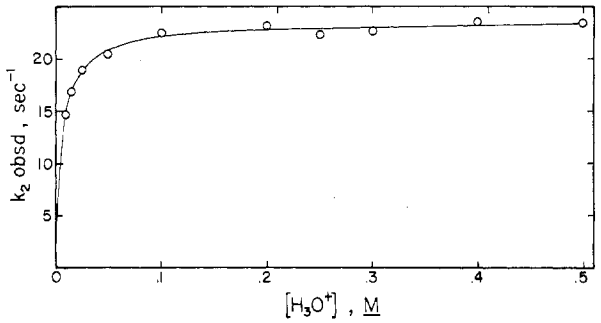


**Figure 6.** Hydrogen ion dependence of $k_2$(obsd). The solid line is calculated from eq 6 where $K_1$ is 165 $M^{-1}$ and $k_2$ is 23.4 $s^{-1}$.

(282 nm). The absorptivity of the triglycine complex at 276 nm is only about 40% of its absorptivity at $\lambda_{max}$ of 300 nm. The rapid addition of this first proton is represented as structure B in Figure 5. Thus the $COO^-$ and $CONH^-$ species are labile in their reaction with $H_3O^+$. For the triglycinamide complex, two first-order reactions are observed after the addition of acid. These have rate constants $k_2'$ and $k_3'$ with $[H^+]$ dependencies very similar to $k_2$(obsd) and $k_3$(obsd) for palladium(II) triglycine.

**Second Reaction of Palladium(II) Triglycine with $H^+$.** Figure 6 shows the variation of $k_2$(obsd) with $H^+$ concentration. The limiting rate at high acidity is typical of the behavior of other metal peptides where the protonation step is fast relative to metal–N(peptide) bond dissociation and it indicates complete formation of the "outside protonated" peptide complex. It is possible to fit the observed kinetics to a single protonated species. The solid line in Figure 6 shows the fit for the mechanism in Figure 5 where $k_2$(obsd) is given by eq 6. The values used for the constants are $K_1 = 165$ $M^{-1}$

$$k_2(\text{obsd}) = \frac{k_2 K_1 [H^+]}{1 + K_1 [H^+]} \qquad (6)$$

and $k_2 = 23.4$ $s^{-1}$. The $K_1$ value gives the $\Delta A_0$ values in Table I if the molar absorptivity of species B corresponds to an absorbance of 0.228 when the initial absorbance of $Pd(H_{-2}GGG)^-$ is 0.401 (i.e., $\Delta A_0 = 0.173$).

From studies of both Ni(II)[11] and Cu(II) complexes,[20] a hydrogen bonded species such as B is expected to have a log $K_H$ value of 4.2. A log $K_H$ value of 2.2 is obtained for the palladium(II)–triglycine complex. This decrease is a result of the energy lost in breaking the Pd(II)–carboxylate bond to form the hydrogen bonded species. Thus the value of the equilibrium between bound and free carboxylate would be approximately $10^2$.

The product of the second reaction would at lower acidities correspond to structure C (Figure 5). The main driving force

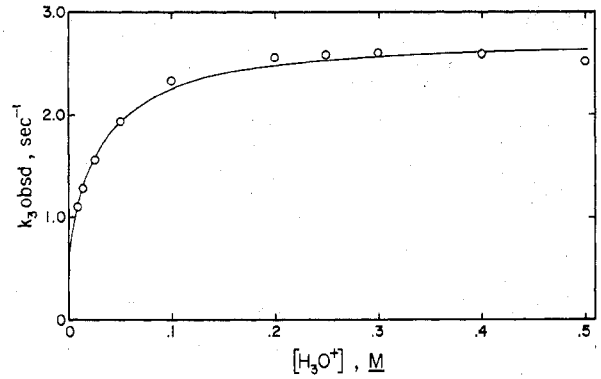


**Figure 7.** Hydrogen ion dependence of $k_3$(obsd). The solid line is calculated from eq 7 where $k_{3d}$ is 0.2 $s^{-1}$, $K_2$ is 34 $M^{-1}$, and $k_3$ is 2.8 $s^{-1}$.

of the reaction to give Y is the rearrangement from an outside-protonated peptide oxygen to a protonated peptide nitrogen with cleavage of the $Pd^{II}$ coordination.

**Third Reaction of Palladium(II) Triglycine with $H^+$.** Figure 7 shows the variation of $k_3$(obsd) with $H^+$ concentration. Again a limiting value is found at high acidity and these data also fit a one-step protonation mechanism in accord with eq

$$k_3(\text{obsd}) = \frac{k_{3d} + k_3K_2[H^+]}{1 + K_2[H^+]} \qquad (7)$$

7 and Figure 5. The constants in eq 7 are resolved and give $k_{3d}$ = 0.2 $s^{-1}$, $K_2$ = 34 $M^{-1}$, and $k_3$ = 2.8 $s^{-1}$.

There is a small difference between the log $K_2$ value of 1.5 for the protonated form of Y (equivalent to $Pd(H_{-1}GGG)H^+$) and the log $K_H$ value of ~2 for the conversion of $Pd(H_{-1}GAG)$ to $Pd(GAG)^+$. However, the driving force for the reaction is the addition of a second proton to give species Z (Figure 5), $Pd(GGG)H^{2+}$.

**Lack of General Acid Catalysis.** The acid dissociation reaction rates of $Pd(H_{-2}GGG)^-$ between pH 2 and 3 were tested for general acid catalysis at various acid concentrations, using $H_3PO_4$ (0.1–1.0 M), $ClCH_2COOH$ (0.05–0.1 M), and citric acid (0.05–0.1 M). There was no observable general acid catalysis by these acids. This is consistent with the proposed mechanisms. The sluggishness of the palladium(II)–peptide complexes makes bond breaking slow compared to proton transfer, thus we see no general acid catalysis. This is in contrast to the behavior of nickel(II) triglycine[11] and copper(II) triglycine[10] where general acids do catalyze the dissociation.

**Summary of the Kinetics and Mechanisms of the Protonation Reactions of Palladium(II) Tripeptides and Tripeptideamides.** (1) The carboxylate group in the $Pd(H_{-2}tripeptide)^-$ complexes and the amide group in the $Pd(H_{-3}GGGa)$ complex are very labile in their reaction with acid. Two factors may contribute to this lability. One is the trans deprotonated peptide group and the other is the size of the $Pd^{II}$ ion which may strain the coordination in these 5,5,5-membered chelate ring systems.

(2) The reactions of acid with the palladium(II) tripeptides proceed in a stepwise unwrapping mechanism (Figure 5) starting at the carboxylate end. Intermediates of appreciable concentration are found containing three nitrogens, two nitrogens, and one nitrogen coordinated to palladium. The cleavage of the peptide–nitrogen–Pd(II) coordinate bonds are many orders of magnitude faster in acid than is the cleavage of the $Pd^{II}$–amine bond (which is the final dissociation step).

(3) The reactions of the Pd–N(peptide) group with acid have a characteristic limiting rate at high $H^+$ concentrations due to 100% protonation of the peptide oxygen (i.e., outside protonation) prior to the Pd–N(peptide) bond cleavage. The outside protonation constants have log $K_H$ values in the range 1.5–2.2. Table III summarizes the equilibrium and rate constants.

**Table III.** Protonation Constants and Rate Constants for $Pd^{II}$(tripeptide) Complexes

| Kinetically determined protonation constants (outside protonation) | Protonated species (structure) | Rate constants, $s^{-1}$ |
|---|---|---|
| log $K_1$ = 2.2 | $Pd(H_{-2}GGG)H$ (X or B) | $k_2$ = 23.4 |
| | $Pd(H_{-1}GGG)$ (C) | $k_{3d}$ = 0.2 |
| log $K_2$ = 1.5 | $Pd(H_{-1}GGG)H^+$ (D) | $k_3$ = 2.8 |

**Table IV.** Protonation Rate Constants for Metal–Triglycine Complexes (Metal = $Cu^{2+}$, $Ni^{2+}$, or $Pd^{2+}$)

| Metal–triglycine complex | $k$, $M^{-1}$ $s^{-1}$ |
|---|---|
| $Cu(H_{-2}GGG)^- + H^+$ | $1 \times 10^7$ [a] |
| $Ni(H_{-2}GGG)^- + H^+$ | $9.5 \times 10^4$ [b] |
| $Pd(H_{-2}GGG)^- + H^+$ | $3.9 \times 10^3$ |
| $Pd(H_{-1}GGG)H^+ + H^+$ | 88 ($K_2k_3$) |

[a] Reference 10. [b] Reference 8.

**Table V.** Log of Protonation Constants for Metal–Tripeptide Complexes (Metal = $Cu^{2+}$, $Ni^{2+}$, or $Pd^{2+}$)

| Metal–tripeptide complex | log $K_H$ | Metal–tripeptide complex | log $K_H$ |
|---|---|---|---|
| $Ni(H_{-1}GGG)$ | 8.8 | $Ni(H_{-2}GGG)^-$ | 7.7 |
| $Cu(H_{-1}GGG)$ | 5.4 | $Cu(H_{-2}GGG)^-$ | 6.6 |
| $Pd(H_{-1}GAG)$ | ~2 | $Pd(H_{-2}GGA)^-$ | 3.2 |

(4) The values of $k_2'$(obsd) for the reaction of the GGGa complex with acid are larger than the corresponding values of $k_2$(obsd) for the GGG complex. This is consistent with the proposed internal hydrogen bonding for the triglycine complex (species B, Figure 5), which cannot be present for the GGGa complex. Protonation of the peptide oxygen weakens the Pd–N(peptide) bond to a greater extent when the proton is not shared by internal hydrogen bonding with a carboxylate group. The same type of effect was found[11] for the reactions of $Ni^{II}(H_{-3}GGGa)^-$ compared to $Ni^{II}(H_{-3}GGGG)^{2-}$. On the other hand, the values for $k_3'$(obsd) for the GGGa complex are essentially the same as the values of $k_3$(obsd) for the corresponding reaction of GGG. Thus, the reactivity of species D in Figure 5 is little affected by the presence of a terminal carboxylate group or terminal amide.

**Comparison of $Pd^{II}$, $Ni^{II}$, and $Cu^{II}$ Peptide Kinetics and Thermodynamic Stabilities.** Table IV gives the second-order rate constants for $H_3O^+$ reaction with various metal–peptide complexes. For the triglycine complexes there is a regular trend in the reactivities with $Cu^{II} > Ni^{II} > Pd^{II}$, covering a range of more than 3 orders of magnitude for similar species. This kinetics behavior follows the relative rates of substitution of these metal ions rather than the basicity of the deprotonated peptide group. The relative basicities [i.e., for $M(H_{-2}GGG)^- + H^+ \rightleftarrows M(H_{-1}GGG)$] are $Ni^{II} > Cu^{II} > Pd^{II}$ as seen in Table V. It is proposed that the rate-determining step in these reactions involves some degree of metal–N(peptide) bond cleavage.

Table V gives the protonation constants of the triglycine complexes and in the case of $Pd^{II}$ values obtained from the CD studies with various L-alanyl substituted complexes. The deprotonated forms of the tripeptides with $Pd^{II}$ compared to $Ni^{II}$ are favored by 4–7 orders of magnitude demonstrating the thermodynamic stability of the Pd–N(peptide) bonding.

**Acknowledgment.** This investigation was supported by Public Health Service Grant No. GM-12152 from the Na-

tional Institute of General Medical Sciences and by National Science Foundation Grant CHE 74-00043.

**Registry No.** GGG, 556-33-2; GGGa, 35790-47-7; AGG, 19729-30-7; GAG, 3146-40-5; GGA, 16422-05-2; Pd, 7440-05-3; Ni, 7440-02-0; Cu, 7440-50-8.

## References and Notes

(1) H. C. Freeman in "The Biochemistry of Copper", J. Peisach, P. Aisen, and W. E. Blumberg, Ed., Academic Press, New York, N.Y., 1966.
(2) H. C. Freeman, *Adv. Protein Chem.*, **22**, 257 (1967).
(3) H. C. Freeman, J. M. Guss, and R. L. Sinclair, *Chem. Commun.*, 485 (1968).
(4) E. W. Wilson, Jr., and R. B. Martin, *Inorg. Chem.*, **9**, 528 (1970).
(5) T. P. Pitner, E. W. Wilson, and R. B. Martin, *Inorg. Chem.*, **11**, 738 (1972).
(6) A review of the structures, equilibria and kinetics of metal peptide complexes is given: D. W. Margerum and G. R. Dukes, "Metal Ions in Biological Systems", Vol. 1, H. Sigel, Ed., Marcel Dekker, New York, N.Y., 1974, Chapter V.
(7) E. J. Billo and D. W. Margerum, *J. Am. Chem. Soc.*, **92**, 6811 (1970).
(8) C. E. Bannister and D. W. Margerum, to be submitted for publication.
(9) C. F. V. Mason, P. I. Chamberlain, and R. G. Wilkins, *Inorg. Chem.*, **10**, 2345 (1971).
(10) G. K. Pagenkopf and D. W. Margerum, *J. Am. Chem. Soc.*, **90**, 501, 6963 (1968).
(11) E. B. Paniago and D. W. Margerum, *J. Am. Chem. Soc.*, **94**, 6704 (1972).
(12) M. T. Barnet, H. C. Freeman, D. A. Buckingham, I. Hsu, and D. van der Helm, *Chem. Commun.*, 367 (1970).
(13) H. L. Grube in "Handbook of Preparative Inorganic Chemistry", 2nd ed, G. Brauer, Ed., Academic Press, New York, N.Y., 1963, p 1584.
(14) H. Flaschka, *Mikrochim. Acta*, 226 (1953).
(15) B. G. Willis, J. A. Bittikofer, H. L. Pardue, and D. W. Margerum, *Anal. Chem.*, **42**, 1340 (1970).
(16) A Purdue University Computing Center modification of D. W. Marquardt's nonlinear least-squares program (SHARE program no. 3094).
(17) M. J. Milano, H. L. Pardue, T. Cook, R. E. Santini, D. W. Margerum, and J. M. T. Raycheba, *Anal. Chem.*, **46**, 374 (1974).
(18) M. J. Milano and H. L. Pardue, *Anal. Chem.*, **47**, 25 (1975).
(19) T. P. Pitner, E. W. Wilson, and R. B. Martin, *Inorg. Chem.*, **11**, 738 (1972).
(20) L. F. Wong, J. C. Cooper, and D. W. Margerum, *J. Am. Chem. Soc.*, **98**, 7268 (1976).

Contribution from the Department of Chemistry, Yale University, New Haven, Connecticut 06520

# Studies of the Reactions of Amines with Carbonyl Functions in Some Cyclopentadienyltungsten Carbonyl Complexes

RICHARD D. ADAMS,* DANIEL F. CHODOSH, and NANCY M. GOLEMBESKI

*Received June 10, 1977*

The compounds $(\eta^5\text{-}C_5H_5)W(CO)_3(CH_2COCH_3)$, I, and $(\eta^5\text{-}C_5H_5)W(CO)_3(COCH_3)$, II, have been investigated in their reactivity toward primary amines. I reacts with methylamine to form the compound $(\eta^5\text{-}C_5H_5)W(CO)_2(NH_2CH_3)(CONHCH_3)$, III, which was characterized by x-ray crystallographic methods. III crystallizes in the space group $P2_1/c$ [$C_{2h}^5$; No. 14]. At −26 °C, $a$ = 10.775 (10), $b$ = 17.807 (17), $c$ = 12.858 (12) Å, $\beta$ = 97.27 (3)°, $\rho_{calcd}$ = 2.14 g cm$^{-3}$, $\rho_{obsd}$ = 2.13 g cm$^{-3}$ (at +20 °C), and $Z$ = 8. III contains a normal $\eta^5$-cyclopentadienyl ring, two linear carbonyl groups, a coordinated methylamine ligand, and an *N*-methylcarbamoyl ligand. The metal-coordinated methylamine ligand is labile and is readily displaced by neutral donor ligands to form the new molecule $(\eta^5\text{-}C_5H_5)W(CO)_2L(CONHCH_3)$, where L = $CNCH_3$ and $P(C_6H_5)_3$. Complex II reacts with the primary amines $RNH_2$ (R = $CH_3$ and c-$C_6H_{11}$) to form $(\eta^5\text{-}C_5H_5)W(CO)_3H$ and the corresponding amide. The reactions of I evidently proceed smoothly through amine attack on the carbon monoxide ligands; however, the preferred site of attack in II appears to have shifted to the acetyl ligand.

## Introduction

The carbonyl function is one of the most ubiquitous and chemically useful atomic groupings known to chemistry. In organic molecules it possesses the general form **1**, while in

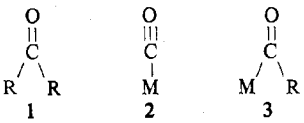

**1** **2** **3**

organometallic complexes it is represented by the linear end-on coordination of the carbon monoxide molecule, **2**. A combination of these two forms yields the organometallic acyl function, **3**.

A principal form of their reactivity is nucleophilic attack at the carbon atom. For example, primary amines readily attack organic ketones (**1**) to produce imines through the classic Shiff-base condensation reaction (1).[1] Metal carbonyls

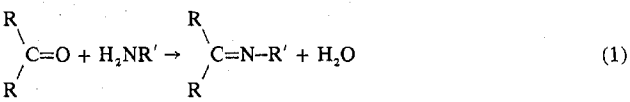

(1)

are also susceptible to nucleophilic attack by amines and produce metal carbamoyl complexes according to reaction 2.[2]

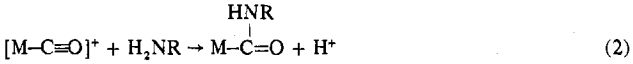

(2)

The reaction of the organometallic acyl function with amines has not been thoroughly investigated, although Heck has reported the formation of amides in the reaction of acyltetracarbonylcobalt compounds with nucleophilic amines.[3]

Studies of the reactivities of the various carbonyl functions as they occur in polyfunctional compounds have been wide and varied. For example, methoxide ion is known to react with acetylpentacarbonylmanganese through attack at the acyl carbon. This leads to formation of methyl acetate and pentacarbonylmanganate(I) anion.[4] On the other hand, methyllithium reacts with benzoylpentacarbonylmanganese through attack on a carbon atom of one of the cis-coordinated carbon monoxide ligands and produces *cis*-acetylbenzoyltetracarbonylmanganate(I) anion.[5] Theoretical considerations of coordinated carbon monoxide, acyl, and carbene functions have shown that the site of attack may be correlated with energy of the lowest unoccupied molecular orbital in the complex.[6] These calculations verified the high reactivity of the coordinated carbene but failed to provide a useful distinction between the acyl and carbon monoxide ligands.

Here, we wish to report the results of our studies of the reactions of primary amines with the carbonyl functions **1**–**3** as they occur in some cyclopentadienyltricarbonyltungsten complexes. This has been achieved by employing the complex $(\eta^5\text{-}C_5H_5)W(CO)_3(CH_2COCH_3)$, I, which contains both type **1** and **2** carbonyl functions and $(\eta^5\text{-}C_5H_5)W(CO)_3(COCH_3)$,

0020-1669/78/1317-0266$01.00/0 